View metadata, citation and similar papers at core.ac.uk

brought to you by CORE

provided by ePrints@Bangalore University

Artificial Cells, Nanomedicine, and Biotechnology

An International Journal

ISSN: 2169-1401 (Print) 2169-141X (Online) Journal homepage: http://www.tandfonline.com/loi/ianb20

A novel amperometric catechol biosensor based on α-Fe_2O_3 nanocrystals-modified carbon paste electrode

C. Sarika, M. S. Shivakumar, C. Shivakumara, G. Krishnamurthy, B. Narasimha Murthy & I. C. Lekshmi

To cite this article: C. Sarika, M. S. Shivakumar, C. Shivakumara, G. Krishnamurthy, B. Narasimha Murthy & I. C. Lekshmi (2016): A novel amperometric catechol biosensor based on α-Fe_2O_3 nanocrystals-modified carbon paste electrode, Artificial Cells, Nanomedicine, and Biotechnology, DOI: 10.3109/21691401.2016.1167702

To link to this article: http://dx.doi.org/10.3109/21691401.2016.1167702

Published online: 11 Apr 2016.

Submit your article to this journal

View related articles

View Crossmark data

Full Terms & Conditions of access and use can be found at
http://www.tandfonline.com/action/journalInformation?journalCode=ianb20

Download by: [Orta Dogu Teknik Universitesi] **Date:** 12 April 2016, At: 17:21

ARTIFICIAL CELLS, NANOMEDICINE, AND BIOTECHNOLOGY, 2016
http://dx.doi.org/10.3109/21691401.2016.1167702

Taylor & Francis
Taylor & Francis Group

A novel amperometric catechol biosensor based on α-Fe_2O_3 nanocrystals-modified carbon paste electrode

C. Sarika[a], M. S. Shivakumar[b], C. Shivakumara[c], G. Krishnamurthy[d], B. Narasimha Murthy[a] and I. C. Lekshmi[a]

[a]Department of Chemistry, CMR Institute of Technology, Bangalore, India; [b]Department of Chemistry, ACS College of Engineering, Bangalore, India; [c]Solid State & Structural Chemistry Unit, Indian Institute of Science, Bangalore, India; [d]Department of Studies in Chemistry, Bangalore University, Bangalore, India

ABSTRACT

In this work, we designed an amperometric catechol biosensor based on α-Fe_2O_3 nanocrystals (NCs) incorporated carbon-paste electrode. Laccase enzyme is then assembled onto the modified electrode surface to form a nanobiocomposite enhancing the electron transfer reactions at the enzyme's active metal centers for catechol oxidation. The biosensor gave good sensitivity with a linear detection response in the range of 8–800 μM with limit of detection 4.28 μM. We successfully employed the sensor for real water sample analysis. The results illustrate that the metal oxide NCs have enormous potential in the construction of biosensors for sensitive determination of phenol derivatives.

ARTICLE HISTORY
Received 31 January 2016
Revised 12 March 2016
Accepted 15 March 2016
Published online 5 April 2016

KEYWORDS
Amperometric biosensing; enzyme; metal-oxide nanocrystals; phenolic detection

Downloaded by [Orta Dogu Teknik Universitesi] at 17:21 12 April 2016

Introduction

Phenol and its derivatives are an important category of compounds, whose presence and concentration levels in community water need to be strictly monitored as they are toxic, and can cause damage to brain, liver, kidneys, muscles, and eyes (Schweigert et al. 2001, Zhou et al. 2013). Toxicity of phenolic compounds also provokes mutagenesis and carcinogenesis in human and other living organisms. These water contaminants come from both nature and industry sources (Karim and Fakhruddin 2012) that include textile, coal, chemical, petrochemical, pharmaceutical, mining, pulp, and paper industries (Decker et al. 2007). They are also used in the manufacture and processing of fertilizers, herbicides, detergents, explosives, preservatives, and solid waste combustion that find their way into the water cycle and ecosystem as a result of the drainage off the community and industrial sewage into river and other surface waters. Another significant and varied applicability is in food quality analysis, where the estimation of polyphenol contents is performed as the food composition undergoes light transformation during post-harvest and processing. The monitoring of polyphenol levels enables food quality control, freshness, and evaluation of antioxidant content (Eremia et al. 2013).

Standard methods generally used for quantitative phenol measurement are high performance liquid chromatography, electrochemical capillary electrophoresis, gas chromatography, and colorimetric spectrophotometry (Alcudia-Leon et al. 2011, Sanchez-Avila et al. 2011). Although these methods give accurate results at low phenol concentrations, they require complicated pretreatment processes and time-consuming detection methods, because of which their use in online monitoring systems is highly restricted. Moreover, these instruments are highly expensive and lack selectivity. Due to these disadvantages, researchers have focused on amperometric biosensors as an alternative detection method, particularly redox enzyme-based biosensors, for measuring phenolic compounds. The amperometric biosensors show good selectivity and moderate operational potentials with working possibility in aqueous medium, applicability to multicomponent solutions, fast response, portability, low cost, and amenability to miniaturization and automation (Goode et al. 2015, Sharma and Mutharasan 2013).

Amperometric biosensors for phenol and diphenol detection are generally prepared with working electrodes having redox enzymes incorporated such as polyphenol oxidases (laccase and tyrosinase) and horseradish peroxidase (Karim and Fakhruddin 2012, Sołoducho and Cabaj 2013). The use of these enzymes on commonly used carbonaceous electrodes helps in lowering their working voltage, thereby minimizing the possibility of dimerization or polymerization of organic analytes to be detected and reduce the production of other electroactive species (Fujita et al. 2014). These side reactions generally passivate the electrode surface or cause higher than expected current levels, which are not desirable. Enzyme-modified carbon electrodes show good sensitivity to selected compound detection depending on the enzyme immobilized and the subsequent biochemical and electrochemical

CONTACT Indira Chaitanya Lekshmi ic.lekshmi@gmail.com, chaitanya.l@cmrit.ac.in Department of Chemistry, CMR Institute of Technology, Bangalore-560 037, India

Supplemental data for this article can be accessed here.

© 2016 Informa UK Limited, trading as Taylor & Francis Group

Downloaded by [Orta Dogu Teknik Universitesi] at 17:21 12 April 2016

reactions (Ciucu 2014). Among the polyphenol oxidases, laccase (p-diphenol: dioxygenoxidoreductases EC 1.10.3.2) is a multicopper enzyme produced by plants and microorganisms (Piontek et al. 2002). The copper atoms at the enzyme active sites are arranged as mononuclear and trinuclear clusters (Type 1 and Type 2/Type 3 sites, respectively), and they reduce atmospheric molecular oxygen directly to water in a four-electron step transfer between the Cu sites without the intermediate formation of soluble H_2O_2. This occurs at the expense of one-electron oxidation of variety of substrates that include phenols and polyphenols (Claus 2004) and the detection of the quinone product generated can be done by electrochemical or amperometric techniques on the electrode surface (Li et al. 2014). For such enzyme-based biosensors, the stabilization of enzymatic activity on the biological recognition element is of great importance. It is generally acknowledged that an effective immobilization technique is a key step to achieve quality construction of the biosensors (Li et al. 2012). The varying levels in activity and the diffusion limitations occurring due to immobilization are mainly dependent on the properties of the support material and the immobilization methods used (Khan and Alzohairy 2010, Krajewska 2004).

Over the past decades, different nanosized materials and metal oxide nanocrystals (NCs) have attracted extensive interests in basic scientific research as well as potential technological applications due to their significant optical, magnetic, and electronic properties. The interesting size and shape dependence of their physicochemical properties make them suitable for a wide variety of applications such as catalysis, organic light-emitting diodes, electrochemical energy storage, and sensors. Among them, metal oxides NCs have high surface area, good biocompatibility, chemical stability, and display fast electron transfer ability (Valentini and Palleschi 2008). The latter features particularly improve their sensitivity to biomolecule detection and offers an ideal immobilization platform, and therefore can be successfully used in electrochemical biosensing (Alkasir et al. 2010, Zhao et al. 2010). Among the differently sized iron oxide NCs developed for biomedical and sensing applications, the most frequently used materials are maghemite (γ-Fe_2O_3) and magnetite (Fe_3O_4) due to their biocompatibility (Aphesteguy et al. 2010, Podzus et al. 2009). Podzus et al. used iron oxide-based chitosan magnetic microspheres with glutaraldehyde as crosslinker to identify and absorb toxic metals in waste water. Li et al. studied on synthesis and use of polydopamine-laccase-Fe_3O_4 magnetic polymeric bionanocomposites on magnetic Au electrode for biosensing of hydroquinone in aqueous solution giving excellent sensitivity, selectivity, and stability. Nanosized particles of magnetite and NiCuZn-doped magnetites were prepared by coprecipitation and sol–gel combustion methods by Aphesteguy et al. and studied for effects of the doping cations on the morphology, structure, and magnetic properties of the resulting spinel to be used in above applications. Nanostructured haematite (α-Fe_2O_3) is another prominent iron oxide phase useful in biomedicine and clinical diagnosis due to its stability under physiological conditions (Laurent et al. 2008, Osaka et al. 2006). α-Fe_2O_3 is a cheap semiconductor material (*n*-type, Eg = 2.1 eV) and one of the most environmental friendly available. Umar et al. (2014) developed a cholesterol biosensor based on cholesterol oxidase coimmobilized with α-Fe_2O_3 micro-pine shaped hierarchical structures that showed high reproducible sensitivity of 78.56 $\mu A/mMcm^2$ and detection limit of 0.018 mM due to high affinity between the cholesterol and ChOx immobilized on α-Fe_2O_3. However, this is one of the few studies available on enzyme immobilized α-Fe_2O_3 nanomaterials for sensitive and selective biosensors.

From the viewpoint of the applied research, different forms of iron (III) oxides are some of the most commonly investigated and used metal oxides for various environmental and industrial applications. As NCs, iron oxide exhibits unique functional features that strongly differ from those of well-crystallized particles and find important applications in nanoelectronic devices, information storage, magnetocaloric refrigeration, color imaging, bioprocessing, ferrofluid technology, and catalysis (Zboril et al. 2002). They are also earth-abundant oxides, extremely stable, and can be easily recycled compared to costlier palladium, rhodium, ruthenium, and iridium particles. Moreover, the durability and copious supply of iron oxides coupled with their environmentally benign nature and low toxicity make them ideal sensing materials and catalysts for sustainable and cost-effective chemical processes (Jagadeesh et al. 2013). In this paper, we have developed a new biosensor based on α-Fe_2O_3 NC-modified carbon-paste electrode with laccase enzyme for amperometric detection of the catechol. The analytical performance factors and the application of the developed catechol biosensor to real samples are investigated. To the best of our knowledge, this is the first report on the use of α-Fe_2O_3 NCs for the fabrication of highly sensitive and selective catechol biosensors.

Experimental

Chemicals and reagents

Laccase (from *Trametes versicolor*) having specific activity of 10 IU mg^{-1} was procured from Sigma, USA. Catechol, 2-chlorophenol, 2-nitrophenol, guaiacol, catechin, ferric nitrate hexahydrate, ethylene glycol, graphite powder, and silicon oil were purchased from SD Fine Chem Ltd. India. Glutaraldehyde, bovine serum albumin (BSA), disodium monohydrogen phosphate heptahydrate, and potassium dihydrogen phosphate were acquired from Hi media, India. All solutions used for analysis were prepared with doubly distilled water.

Synthesis and characterization of α-Fe_2O_3 NCs

α-Fe_2O_3 NCs were synthesized by sol-gel method using ethylene glycol as solvent following the procedure adopted by Xu et al. (2007). 16 g ferric nitrate was firstly dissolved in 100 ml solvent with vigorous stirring for 2 h at 40 °C, and then the obtained sol was heated to 80 °C and kept at that temperature for 2 h until a brown gel was formed. The gel was aged for 2 h followed by drying at 170 °C for 16 h. After drying, the xerogel was annealed at 410 °C in air. The crystal growth of α-Fe_2O_3 NCs prepared was analyzed from powder X-ray diffraction (XRD) patterns recorded from 10° to 80° with a PANalytical Empyrean diffractometer using Cu Kα

Downloaded by [Orta Dogu Teknik Universitesi] at 17:21 12 April 2016

($\lambda = 1.5418$ Å) radiation and with a Nickel filter. The TEM images of α-Fe_2O_3 NCs were recorded using JEOL JEM-2100F Field Emission microscope operating at an accelerating voltage of 200 kV. The samples for the TEM analyses were prepared by adding a drop of NC solution onto carbon-coated copper grids and allowing the solvent to evaporate. NC solution was prepared by vigorous sonication of NC powder in isopropanol as solvent for 15 min.

Preparation of bare and modified carbon-paste electrodes

Bare and NC-modified carbon-paste electrodes were constructed for enzyme immobilization and resultant electrochemical studies. For bare carbon-paste electrode (BCPE) construction, the carbon paste was prepared by grinding graphite powder (70% w/w) with silicon oil (30% w/w) until a homogeneous paste was obtained. For α-Fe_2O_3 NC-modified carbon-paste electrode (α-Fe_2O_3 NCs–CPE), Fe_2O_3 NCs were added to graphite powder in different weight ratios of 1:2, 1:3, 1:4, and 1:5 (w/w) followed by the addition of silicon oil and mixed thoroughly to a uniform paste. For immobilization of the laccase enzyme onto α-Fe_2O_3 NCs incorporated carbon-paste electrode (Lac–α-Fe_2O_3 NCs–CPE), the enzyme solution containing 5 IU laccase, 20 µl of glutaraldehyde (5% (v/v)), and 2.5 mg of BSA were added into specific α-Fe_2O_3NC-graphite powder mixture. Finally, carbon paste was obtained by mixing with 10 µl of silicon oil for 20 min in all cases. The different pastes were firmly placed in cavities of Teflon tube with 2-mm internal diameter and containing copper rod on one end. The surface of the nanocomposite electrode at the other end was smoothened by a wax paper before starting the electrochemical experiments. The obtained electrodes were stored in the refrigerator at 4 °C, when they were not in use. The prepared nanocomposites of Lac–α-Fe_2O_3NCs–CPE together with Lac-BSA-glutaraldehyde system were characterized by a Fourier transform IR spectroscopy using Perkin Elmer FTIR/FIR Spectrometer, Frontier using KBr as a reference in the range of $4000 - 400\,cm^{-1}$.

Electrochemical measurements

The electrochemical experiments were performed with an Autolab PGSTAT 3.0 Potentiostat/Galvanostat with a conventional three-electrode system. The carbon-paste electrode, a Pt wire, and a calomel electrode were used as the working electrode, auxiliary electrode, and the reference electrode, respectively. All measurements were carried out at room temperature. The electrochemical behavior of α-Fe_2O_3 NCs–CPE was examined by cyclic voltammetry (CV) in 0.1 M of KCl solution containing 10-mM $Fe(CN)_6^{3-/4-}$ and was compared with those of BCPE. CVs were recorded in the potential range between −0.2 V and 0.8 V at 50 mV s^{-1} scan rate. The electrocatalytic activity of the α-Fe_2O_3NCs–CPE and laccase immobilized α-Fe_2O_3NCs–CPE were investigated in the absence and presence of 1-mM catechol in 0.2 M of phosphate-buffered saline (PBS) also by CV measurements at a pH of 7.0. The CVs for this were recorded in the potential range between −0.2 V and 0.8 V at 50 mV s^{-1} scan rate. The influence of the pH was checked in 0.2 M of PBS with 400-µM catechol in the range of pH 5.0–9.0. The pH values of the buffer solutions were measured with a Systronics-model pH meter equipped with a glass electrode. The dependency of the steady-state amperometric response on the working potential was carried out in 0.2 M of PBS at pH 7.0 in the voltage range of 0.2 to 0.4 V with catechol increments from 200 to 600 µM. Similarly, to determine optimum temperature for measurements, 400 µM of catechol in 0.2-M PBS at pH 7.0 was incubated in the temperature range 25–60 °C with a stepwise increase of 5 °C. The steady-state amperometric responses of the Lac-α-Fe_2O_3NCs–CPE at different catechol concentrations were determined by the successive addition of different volumes of 2 and 200-mM catechol into 20 ml of PBS with stirring under the optimum potential of 0.3 V vs. Hg/Hg_2Cl_2. For this, first the enzyme electrode was equilibrated in 0.2 M of PBS at 0.3 V, until a constant current ($i1$) called background current was obtained. Then, aliquots of catechol solution were added to the electrochemical cell. The steady-state current response ($i2$) to the addition of catechol was recorded and the current difference ($\Delta i = i2 - i1$) was determined. A calibration curve of Δi-catechol concentration was then plotted. Five biosensors were prepared under the same conditions independently to study the electrode-to-electrode reproducibility. The long-term stability of Lac-α-Fe_2O_3NCs–CPE was determined by performing activity assays within 20 days. The electrodes were stored in dry atmosphere at 4 °C when not in use.

To demonstrate the practical application of the biosensor, we also investigated the response of the sensor in real water samples. The water from the tap and industry effluents was used for the analysis after filtration with a 0.2-µM membrane. Each sample was added to 0.2 M of PBS solution for 2-fold dilution at pH 7.0, and on attaining current stability, amperometric detection by the Lac-α-Fe_2O_3NCs–CPE was performed using 100-µM catechol at 0.3 V. The experiments were repeated for five times. Initially, electrochemical impedance measurements were also carried out to analyze the charge transfer properties of bare and modified carbon-paste electrodes using CHI604E electrochemical work station. A platinum foil was used as the counter electrode and Ag/AgCl as reference electrode, and measurements were carried out at room temperature.

Results and discussion

Preparation and structural characterization of α-Fe_2O_3 NCs and modified CPEs

α-Fe_2O_3 NCs were synthesized by sol-gel method using ferric nitrate precursor and ethylene glycol as solvent. Careful experiments were done to optimize the heating temperatures and minimize the interference of moisture which was found to have profound influence on the phases of iron oxide formed. The formation of different iron oxide phases was avoided since they had widely varying conductivity and magnetic features. The growth and crystallinity of α-Fe_2O_3 NCs were confirmed by recording XRD pattern and the result for polycrystalline NCs is shown in Figure 1. Well-defined

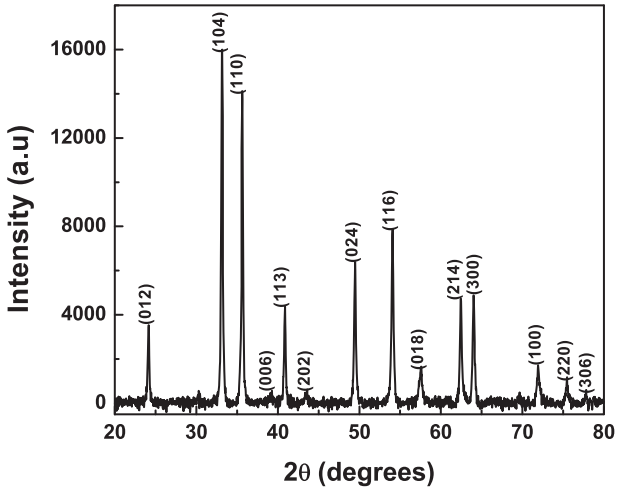

Figure 1. XRD pattern of crystalline α-Fe_2O_3 NCs prepared by sol-gel method.

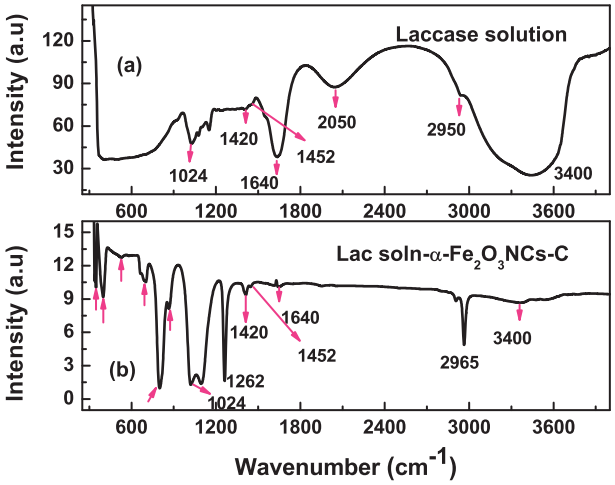

Figure 2. FT-IR spectra of laccase solution (a), and laccase immobilized α-Fe_2O_3NCs-CPE (b) showing formation of nanobiocomposite.

diffraction peaks were seen at 24.4°, 33.1°, 35.6°, 39.3°, 40.8°, 43.3°, 49.4°, 54.1°, 57.6°, 62.4°, 64.1°, 71.9°, 75.47°, and 77.7° corresponding to (012), (104), (110), (006), (113), (202), (024), (116), (018), (214), (300), (100), (220), and (306) Bragg reflections, respectively. The reflection planes are consistent with the standard pattern for α-Fe_2O_3 reported. The average particle size of α-Fe_2O_3 NCs was estimated using the Debye–Scherrer equation taking full-width at half maximum of the highest intensity diffraction peak and was found to be 39 nm. TEM image was obtained for the NCs and was seen as aggregated into small cluster-like structures, which could be due to the accumulation of NCs synthesized devoid of capping ligands. Such accumulation is known (Claridge et al. 2009, Xuan et al. 2009) and occurs due to charges on NC surfaces which cause to attract each other. From the aggregated TEM image, the particle size could be approximately determined and found to be in agreement with the value obtained from X-ray diffraction analysis. The TEM image (see Supplementary Figure S1) is given as supplementary information. The inset of the figure shows high resolution image of a NC and the interplanar distance measuring adjacent lattice fringes in the image is about 0.251 nm corresponding to (110) plane of α-Fe_2O_3.

α-Fe_2O_3 NCs were further mixed with graphite powder in different weight ratios and made into a paste with silicon oil for preparation of modified carbon-paste electrode. NC weight ratios were optimized to achieve maximum sensitivity for the biosensor to be prepared. Further, the laccase enzyme was immobilized along with stabilizing and cross-linking agents such as BSA and glutaraldehyde and packed in Teflon tube to fabricate amperometric biosensors. Bifunctional agents such as glutaraldehyde cross-link with the reactive amino groups of enzymes (Gao et al. 2013). The incorporation of BSA along with glutaraldehyde during the process of enzyme immobilization through hydrophobic interactions, contributed to the long-term operational stability of the enzyme biosensor. This was investigated in our previous studies on laccase-based sensors for the analysis of substituted phenols (Sarika et al. 2015a).

We have optimized the concentrations of laccase, BSA, and glutaraldehyde combination for maximum biosensor response with minimum reagent levels using Box–Behnken design of experiment (Sarika et al. 2015b). The modified electrodes and enzyme immobilization were analyzed using FT-IR spectroscopy for binding sequence and biocomposite formation. Figure 2 shows FT-IR spectra recorded for laccase solution (a) and for lac soln-α-Fe_2O_3 NC-C paste (b), where laccase solution in both cases refers to combination of laccase, BSA, and glutaraldehyde solutions in required proportion as mentioned in the experimental section. The modified carbon paste sample shown in Figure 2 has α-Fe_2O_3 to carbon ratio of 1:4.

The FT-IR spectra for α-Fe_2O_3-modified carbon paste show multiple bands in the region between 350 and 700 cm^{-1} corresponding to Fe-O stretching and bending vibration modes. They could be attributed to the dipole moments parallel and perpendicular to "c" plane of hexagonal α-Fe_2O_3 lattice with face-sharing octahedra (Fouda et al. 2013). The multiple peaks lying in the range 700–1100 cm^{-1} could be considered as arising due to Fe-OH and Fe-OH_2 stretching that becomes prominent on adding laccase solution to the α-Fe_2O_3-modified carbon paste. Important peaks relating to α-Fe_2O_3 phase are marked by red downward arrow in Figure 2(b) and are found to be absent in laccase solution spectra. The peaks lying in the range 650–800 cm^{-1} in the composite spectra could also be arising due to out-of-the plane N–H wagging modes (Silverstein et al. 2005). The broad IR peak centered around 3400 cm^{-1} in the laccase solution spectra of Figure 2(a) is due to NH- and OH-stretching vibrations in the enzyme (Li et al. 2014, Mazur et al. 2009), while the peaks at 1420, 1450, and 1640 cm^{-1} correspond to the amide linkages from enzyme and cross-linking agents. The intensity of these laccase solution peaks decreased in the nanocomposite due to their much reduced weight proportion in the carbon-paste matrix compared to the pure solution shown in Figure 2(a). IR absorption bands at 1024 and 1075 cm^{-1} could be attributed to C–N stretching, which is significant for the composite. The peaks around 2950 cm^{-1} could be related to symmetric and asymmetric stretching of NH_3 groups in both the spectra, while the peak at 1262 cm^{-1} could be assigned to C-O stretching vibrations in the nanocomposite. It is noteworthy, that unlike laccase solution spectra, those of Figure 2(b) showed strong signatures of M–O, M–OH, M–OH_2, C–N, and C–O stretching vibrations pointing to the formation of nano-bio-composite.

Downloaded by [Orta Dogu Teknik Universitesi] at 17:21 12 April 2016

Downloaded by [Orta Dogu Teknik Universitesi] at 17:21 12 April 2016

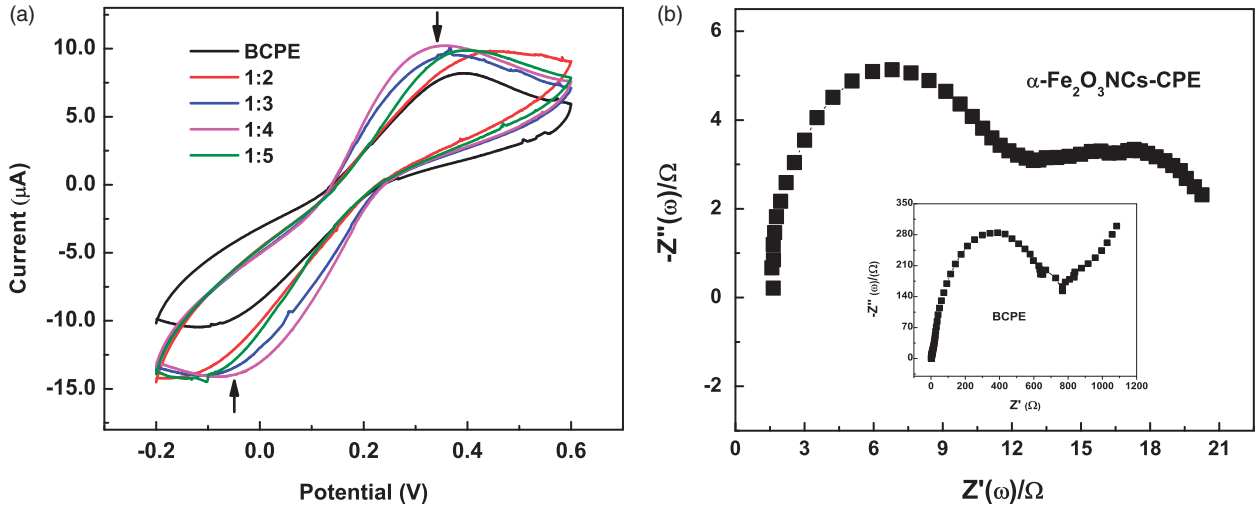

Figure 3. (a) CVs of α-Fe_2O_3 NC-modified CPE and BCPE in 10 mM of $Fe(CN)_6^{3-/4-}$ solution measured at a scan rate of 50 mV s^{-1}; (b) Electrochemical impedance spectra of α-Fe_2O_3NCs–CPE in 10 mM of $Fe(CN)_6^{3-/4-}$ at a polarization potential of 0.2 V in a frequency range of 1–10^6 Hz. Inset shows corresponding spectra of BCPE.

Effect of α-Fe_2O_3 NC loading on the performance of CPE electrode

α-Fe_2O_3 NC loading were earlier analyzed for different weight ratios (1:2, 1:3, 1:4, and 1:5) with respect to graphite powder in order to prepare modified carbon-paste electrodes and the amount of loading was optimized to achieve maximum sensitivity for the amperometric biosensor. The electron transfer features of α-Fe_2O_3 NCs–CPEs at different NC weight ratios were examined by cyclic voltammetry using $Fe(CN)_6^{3-/4-}$ redox probe, and the performances were compared with BCPE, as shown in Figure 3(a). A pair of reversible redox waves by potassium ferrocyanide–ferricyanide solution$^-$ was observed between −0.2 V and 0.6 V at all electrodes with a prominent decrease in the working potential for NC ratio of 1:4. The peak-to-peak potential separation (ΔEp =0.43 V) between the cathodic and anodic waves was also found lowest for the same Fe_2O_3 NC loading, while their anodic and cathodic peak currents were the highest. The ΔEp values for BCPE (0.495V) and α-Fe_2O_3NCs-CPE are comparable to the values reported in literature (Aydogdu et al. 2013, Erdem et al. 2014). The results denoted that adding α-Fe_2O_3 NCs-CPE at 1:4 ratio provided the highest electron transfer at solution/electrode interface due to their improved electrocatalytic and conductivity properties and extended active surface area (Yao and Shiu 2007, Zhang et al. 2009). The redox processes can be achieved at low potential by incorporating metal oxide NCs to carbon-paste electrode, and these experiments were performed at a scan rate of 50 mV s^{-1} which was optimized for the electrochemical experiments in our lab.

Figure 3(b) shows the electrochemical impedance spectra of the α-Fe_2O_3 NCs-CPE electrode together with that of the BCPE (shown in the inset of the figure) in 10-mM solution at a polarization potential of 0.2 V and in the frequency range of 1–10^6 Hz. The electrochemical impedance spectrum analyzes the charge transfer features at an electrode interface with the electrolyte and is dependent on its dielectric and conduction properties. This is particularly useful in studying interface features, when the electrode surface is modified by iron oxide NCs. The charge transfer resistance of the electrode surface to the electrolytic solution is indicated by the diameter of the semicircle in the Nyquist plot, which is remarkably low (almost 60 times less) for Fe_2O_3 incorporated electrode compared to the unmodified one. The semicircle portion of the Nyquist plot corresponds to electron–transfer-limited processes involving the redox probe, and lower resistance value is attributable to increased electron transfer ability of the NC-modified electrode. The observation is in agreement with the cyclic voltammetry studies above. However, a linear region corresponding to diffusion controlled kinetics is observed above 800 ohm for BCPE, which is less pronounced in the case of Fe_2O_3-modified electrode.

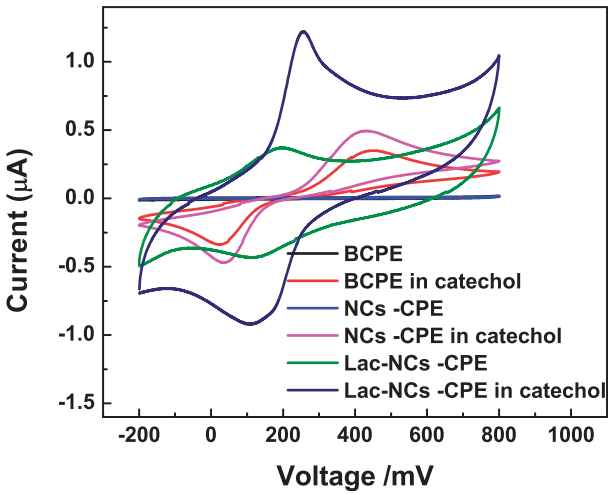

Figure 4. CVs of BCPE, α-Fe_2O_3NCs–CPE, and Lac-α-Fe_2O_3NCs–CPE in presence of 0.2-M pH 7 PBS solution in presence and absence of 1-mM catechol at a scan rate of 50 mV s^{-1}.

Electrocatalytic activity of bare and modified carbon-paste electrodes

Figure 4 depicts cyclic voltammogram of different electrodes in pH-7 PBS solution at a scan rate of 50 mV s^{-1}. No redox peaks are observed for the BCPE demonstrating the electrochemical inertness of the electrode, while very small peaks corresponding to reversible Fe^{2+}/Fe^{3+} redox couples are observed for α-Fe_2O_3NC–CPE between 0.2 and 0.5 V (not seen

Downloaded by [Orta Dogu Teknik Universitesi] at 17:21 12 April 2016

clearly in the graph). However, the voltammogram of Lac-α-Fe_2O_3NCs–CPE shows pairs of well-defined and stable redox peaks with very large increase in current, attributed to the direct electron transfer between the electroactive center of the immobilized laccase and the modified electrode surface. The figure also shows the CVs of different electrodes in 0.2-M PBS solution containing 1-mM catechol. A pair of redox peaks is observed on the BCPE dipped in catechol solution between 0 and 0.45V attributed to the reversible oxidation of catechol. Compared with the BCPE, α-Fe_2O_3NCs–CPE exhibited higher redox peak currents and smaller peak-to-peak separation in catechol due to enhanced electrode surface potential and conductivity of the α-Fe_2O_3NCs dispersed matrix. Laccase immobilization on the electrode displayed very large current flow with additional redox peaks between 0.1 and 0.2 V that needs to be understood better. The area under the CV gets greatly enhanced on adding the phenol demonstrating the highly efficient catalysis by laccase toward catechol oxidation.

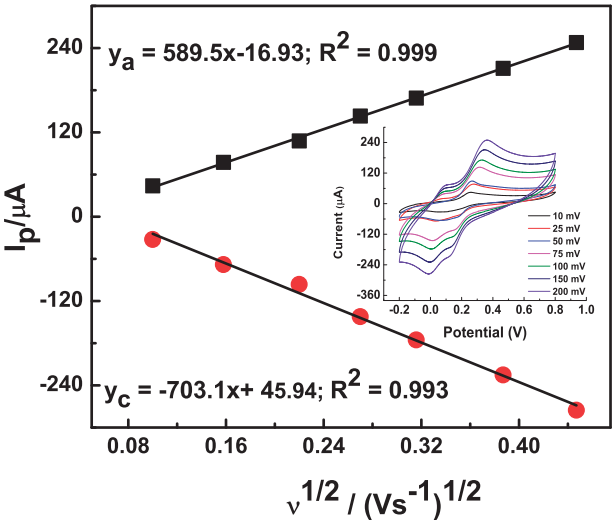

Figure 5. The plot of the peak current vs. the square root of the scan rate for α-Fe_2O_3 NCs–CPE (inset: CVs at different scan rates) in 0.2-M pH 7 PBS solution containing 1 mM of catechol.

The peak-to-peak separation seen here is, however, in agreement with the reported values in literature for enzymes and metal oxide (Erdem et al. 2014).

The effect of scan rate on the voltammetric response of the α-Fe_2O_3NCs–CPE is shown in Figure 5. As the scan rate increases, the peak currents increase while the redox peak potentials shift slightly. The anodic and cathodic peak current values shown in the inset of the figure exhibit a linear dependence on the square root of the scan rates indicating that the mass transfer phenomenon at the electrochemical probe, and the electrode interface is mainly a diffusion-controlled process (Song et al. 2010). The above electrochemical experiments demonstrated that the nanocomposite provides a biocompatible environment for the immobilization of laccase, and that the α-Fe_2O_3NCs facilitated faster electron transfer for laccase. The reaction mechanism is illustrated in the schematic Figure 6. First, the catechol in contact with the laccase is oxidized to 1,2-benzoquinone in the presence of molecular oxygen. Subsequently, the 1,2-benzoquinone is reduced electrochemically on the surface of the electrode. The obtained current in the process of electrochemical reduction of the 1,2-benzoquinone to catechol is proportional to the concentration of the catechol, which is further illustrated in the next section.

To acquire the optimal amperometric response, we also investigated the effects of the solution pH, temperature, and applied potential on the current values. As shown in Figure 7(a), the current value reaches the maximum value at pH 7 and followed by a dramatic decrease. Figure 7(b) presents the influence of different applied potentials on the amperometric responses. It can be clearly seen that the maximum current value occurs when 0.2 M of PBS solution with pH 7 was used, and the applied potential was set at 0.3 V in the experiments. Figure 7(c) presents the influence of temperature on the current responses. The optimal temperature of the biosensor was found to be 40 °C. The results of the study with *Trametes versicolor* species is almost similar as reported in the literature stating that laccase activity is maximum at temperatures between 30 °C

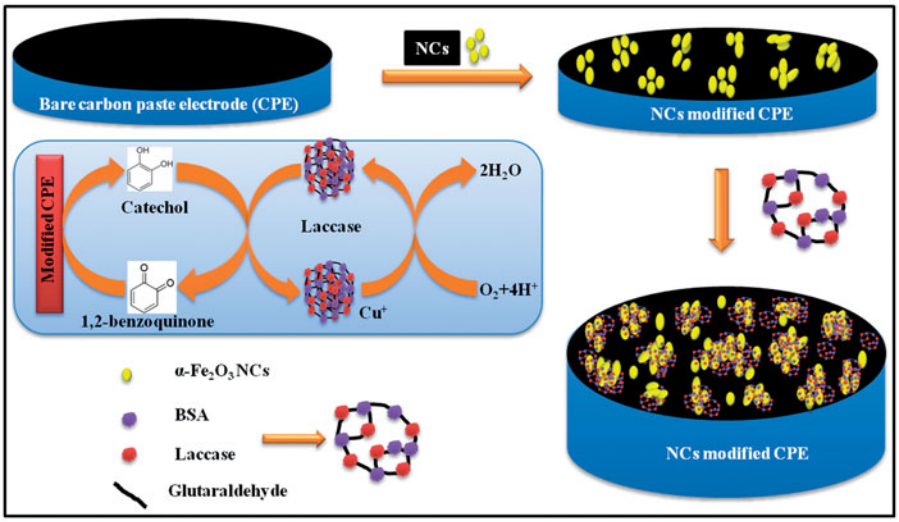

Figure 6. Schematic representation of laccase-catalyzed oxidation of catechol with its subsequent electrochemical reduction on the α-Fe_2O_3 NC-modified CPE.

Downloaded by [Orta Dogu Teknik Universitesi] at 17:21 12 April 2016

and 50 °C for enzymes obtained from sources such as *Trametes hirsuta*, *Sclerotium rolfsii*, and *Pleurotus ostreatus* (Duran et al. 2002).

Amperometric biosensing of catechol

The steady-state amperometric responses of Lac-α-Fe_2O_3NCs–CPE to different concentrations of catechol were analyzed by successive addition of different volumes of 2- and 200-mM catechol into 20 ml of pH-7 PBS solution under the optimized conditions. The steady-state current values gradually increased with the successive addition of catechol, as can be seen from Figure 8(a). The initial step for Lac-α-Fe_2O_3NCs–CPE occurred on adding 8-μM catechol into the PBS solution. The corresponding calibration curves are shown in Figure 8(b). The Lac-α-Fe_2O_3NC–CPE showed a linear range of response between 8 and 800 μM of catechol solution with linearity equation $Y = 0.028x + 0.467$ ($R^2 = 0.992$) and a limit of detection of 4.28 μM ($S/N = 3$). Table 1 compares biosensing performance of several laccase-modified electrodes toward catechol. The biosensor fabricated in this study shows low detection limit, wide linear range, and reasonable sensitivity, considering the ease of preparation and high chemical stability of α-Fe_2O_3.

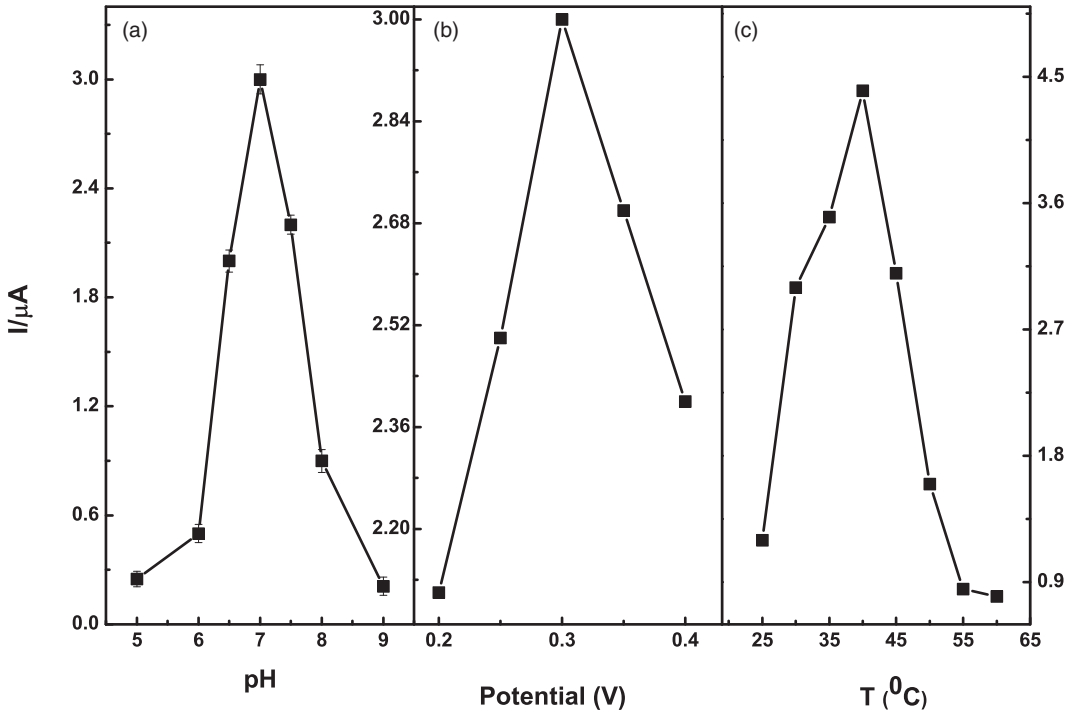

Figure 7. Effect of solution pH (a) applied potential (b) and temperature (c) on the steady-state current response of Lac-α-Fe_2O_3NCs–CPE in 0.2-M pH 7 PBS solution containing catechol.

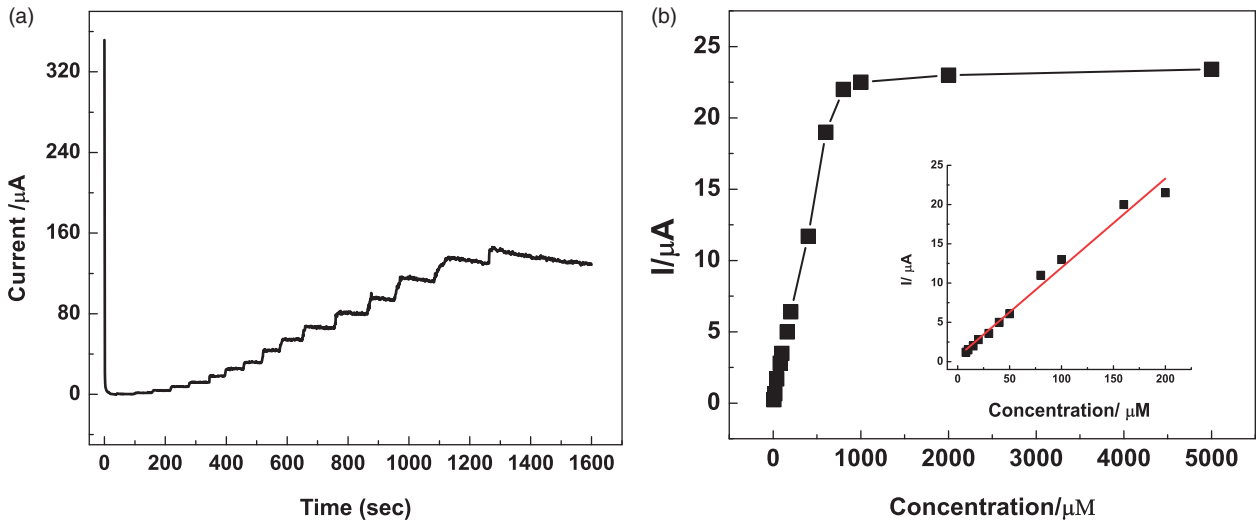

Figure 8. (a) Chronoamperometric responses of Lac-α-Fe_2O_3NCs–CPE on successive addition of different concentrations and volumes of catechol solutions into pH 7, 0.2 M of PBS solution at an applied potential of 0.3 V; (b) Calibration curve with nonlinear fitting for Lac-α-Fe_2O_3NCs–CPE response. Inset: Calibration curve with linear fitting.

Downloaded by [Orta Dogu Teknik Universitesi] at 17:21 12 April 2016

Table 1. A comparison of biosensing properties of various laccase-based catechol biosensors.

Electrode description	Substrate	Detection limit (μM)	Linearity (μM)	Ref.
Laccase/carbon fibres	Catechol	NR	1–90	Freire et al. (2001)
Lac/AP-rGOs/Chit/GCE	Catechol	7	15–700	Zhou et al. (2013)
MB-MCM-41/PVA/lac	Catechol	0.331	4–87.98	Xu et al. (2009)
Laccase/CNTs – CS/GCE	Catechol	0.66	1.2–30	Liu et al. (2006)
PDA-Lac-NiCNFs/MGCE	Catechol	0.69	1–9100	Li et al. (2014)
Lac-α-Fe_2O_3NC-CPE	Catechol	4.28	8–800	This study

Stability and reproducibility of Lac-α-Fe_2O_3NCs–CPE

We studied Lac-α-Fe_2O_3NCs–CPE electrode for good repeatability, reproducibility, and stability and they showed satisfactory behavior. The relative standard deviation (RSD) of the biosensor response to catechol was analyzed and found to be within 3.0% for 10 successive measurements indicating the good repeatability of the biosensor. Five independent biosensors were prepared under the same conditions to study the electrode-to-electrode reproducibility, and the RSD of the electrodes was found to be within 4% indicating that the biosensors also possess good reproducibility. The long-term stability of Lac-α-Fe_2O_3 NCs–CPE was determined by performing activity assays within 20 days. The electrodes were stored in dry atmosphere at 4 °C when not in use during this period. Activity retention of 90% was observed after its 95 uses during the span of 20 days for Lac-α-Fe_2O_3NCs–CPE indicating good storage as well as operational stability of the laccase biosensor. The low activity loss may be attributed to the mild immobilization procedures adopted (i.e. through co-crosslinking method of laccase immobilization with stabilizing agents (Sarika et al. 2015a)) and a beneficial environment for preventing enzyme leakage. Immobilization of laccase in modified carbon-paste matrix has provided a biocompatible microenvironment around the enzyme, which is evident from IR and electrochemical studies. The operational stability is tested and achieved through systematic increase in enzyme loading, which also caused controlled diffusion. The stabilization is achieved due to the newer bonds formed between the enzyme and the support matrix. The developed biosensors have achieved 95% of the steady-state current within 6 s of introduction of sample, which is satisfactory for a biosensor response. For comparison, a response time of 4s ($t_{90\%}$) was reported by Xu et al for laccase immobilized on methylene blue-modified mesoporous silica MCM-41/PVA and Zhou et al reported 5s ($t_{95\%}$) response time for reduced graphene oxide-based biosensor for high-sensitive detection of phenols in water samples. Such a fast response reflects the increased electron transfer processes enabled for laccase enzyme due to NC-modification of the carbon paste.

Selectivity study and real sample analysis

Selectivity of the biosensors was tested and studied using catechol and other phenolic compounds including 2-chlorophenol, 2-nitrophenol, guaiacol, phenol, and catechin (see bar diagram in Figure 9). A response of 100% was obtained for catechol, and the biosensor exhibited poor or no response toward other phenolic compounds. Thus we concluded that the sensor showed excellent selectivity for catechol. We also investigated the response of the biosensor toward real water samples in order to demonstrate its practical application for sensing within a more general analyte. For this, different water samples, including tap water from the lab and textile industry effluents, were filtered and used in presence of a buffer (0.2 M of PBS solution with a pH of 7 resulting in dilution). When the current became stable, amperometric detection was performed by adding catechol to Lac-α-Fe_2O_3NCs–CPE at 0.3 V, and the experiment was repeated five times. The results are illustrated in Table 2. The recovery percentage looks satisfactory in each case confirming the potential application of the biosensor in detecting phenols in real water samples and industrial effluents.

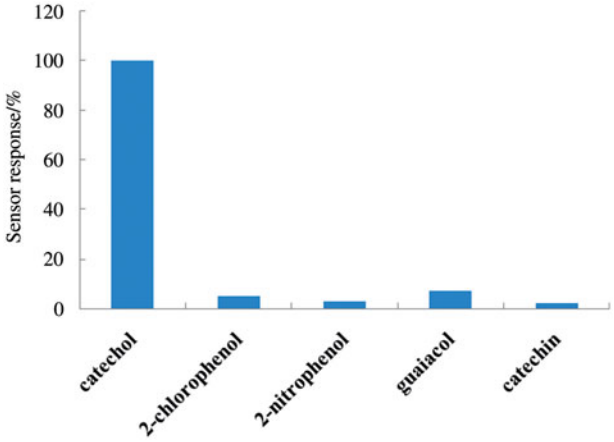

Figure 9. Relative responses of the biosensor for different phenolic compounds including catechol, 2-chlorophenol, 2-nitrophenol, guaiacol, and catechin. A total of 100 μM of the phenol in pH-7 PBS solution is used in all cases.

Conclusions

A novel catechol biosensor was successfully prepared by facile and efficient immobilization of the laccase enzyme on α-Fe_2O_3 NC-modified carbon-paste electrode. Small α-Fe_2O_3 NC aggregates offer large number of active sites for immobilization of the multicopper oxidase enzyme forming a nanobiocomposite, as confirmed from the IR studies. The novel biosensor displayed efficient electrocatalysis toward catechol with wide linear range and low detection limit. The biosensor also showed good repeatability, reproducibility, and storage stability attributed to the biocompatible microenvironment of the composite matrix. The laccase-NC sensor showed very small response time and we could successfully apply the biosensor in detecting catechol in real water samples.

Table 2. Determination of catechol in real water samples.

Sample	C_{added} (μM)	C_{found} (μM)	Recovery (%)
Tap water	100	101.3	101.3
Textile industry effluent 1	100	97.3	97.3
Textile industry effluent 2	100	98	98

Acknowledgements

I.C.L. and C.S. would like to thank Prof. Balaji Jagirdhar and Ms. Ancila Urumese at Indian Institute of Science, Bangalore, for helping us with TEM measurements. C.S., B.N.M., and I.C.L would like to acknowledge Dr. Chithambararaj, research associate with the project for useful discussions and material analysis.

Disclosure statement

The authors declare that they have no conflict of interest in the publication.

Funding information

This work has been financially supported by Department of Science and Technology, Government of India (Grant No. SR/NM/NS-1161/2013).

References

Alcudia-Leon MC, Lucena R, Cardenas W, Valcarcel M. 2011. Determination of phenols in waters by stir membrane liquid – liquid – liquid microextraction coupled to liquid chromatography with ultraviolet detection. J Chromatogr A. 1218:2176–2181.

Alkasir RSJ, Ganesana M, Won YH, Stanciu L, Andreescu S. 2010. Enzyme functionalized nanoparticles for electrochemical biosensors: a comparative study with applications for the detection of bisphenol A. Biosens Bioelectron. 26:43–49.

Aphesteguy JC, Jacobo SE, Schegoleva NN, Kurlyandskaya GV. 2010. Characterization of nanosized spinel ferrite powders synthesized by coprecipitation and autocombustion method. J Alloy Compd. 495:509–513.

Aydogdu G, Zeybek DK, Pekyardimci S, Kilic E. 2013. A novel amperometric biosensor based on ZnO nanoparticles-modified carbon paste electrode for determination of glucose in human serum. Artif Cells Nanomed Biotechnol. 41:332–338.

Ciucu AA. 2014. Chemically modified electrodes in biosensing. J Biosens Bioelectron. 5:154.

Claridge SA, Castleman AW, Jr, Khanna SN, Murray CB, Sen A, Weiss PS. 2009. Cluster-assembled materials. ACS Nano. 3:244–255.

Claus H. 2004. Laccases: structure, reactions, distribution. Micron. 35:93–96.

Decker H, Schweikardt T, Nillius D, Salzbrunn U, Jaenicke E, Tuczek F. 2007. Similar enzyme activation and catalysis in hemocyanins and tyrosinases. Gene. 398:183–191.

Duran N, Rosa MA, D'Annibale A, Gianfreda L. 2002. Applicationsof laccases and tyrosinases (phenoloxidases) immobilized on different supports: A review. Enzym Microb Technol. 31:907–931.

Erdem C, Zeybek DK, Aydogdu G, Zeybek B, Pekyardimci S, Kilic E. 2014. Electrochemical glucose biosensor based on nickel oxide nanoparticle-modified carbon paste electrode. Artif Cells Nanomed Biotechnol. 42:237–244.

Eremia SAV, Vasilescu I, Radoi A, Litescu SC, Radu GL. 2013. Disposable biosensor based on platinum nanoparticles-reduced graphene oxide-laccase biocomposite for the determination of total polyphenolic content. Talanta. 110:164–170.

Fouda MFR, ElKholy MB, Mostafa SA, Hussien AI, Wahba MA, El-Shahat MF. 2013. Characterization and evaluation of nano-sized α-Fe_2O_3 pigments synthesized using three different carboxylic acid. Adv Mat Lett. 4:347–353.

Freire RS, Duran N, Kubota LT. 2001. Effects of fungal laccase immobilization procedures for the development of a biosensor for phenol compounds. Talanta. 54:681–686.

Fujita S, Yamanoi S, Murata K, Mita H, Samukawa T, Nakagawa T, Sakai H, Tokita Y. 2014. A repeatedly refuelable mediated biofuel cell based on a hierarchical porous carbon electrode. Sci Rep. 4:1–8.

Gao W, Bian Y, Chang TM. 2013. Novel nanodimension artificial red blood cells that act as O_2 and CO_2 carrier with enhanced antioxidant activity: PLA-PEG nanoencapsulated PolySFHb-superoxide dismutase-catalase-carbonic anhydrase. Artif Cells Nanomed Biotechnol. 41:232–239.

Goode JA, Rushworth JVH, Millner PA. 2015. Biosensor regeneration: a review of common techniques and outcomes. Langmuir. 31:6267–6276.

Jagadeesh RV, Surkus AE, Junge H, Pohl MM, Radnik J, Rabeah J, et al. 2013. Nanoscale Fe_2O_3-based catalysts for selective hydrogenation of nitroarenes to Anilines. Science. 342:1073–1076.

Karim F, Fakhruddin ANM. 2012. Recent advances in the development of biosensor for phenol: a review. Rev Environ Sci Biotechnol. 11:261–274.

Khan AA, Alzohairy MA. 2010. Recent advances and applications of immobilized enzyme technologies: a review. Res J Biol Sci. 5:565–575.

Krajewska B. 2004. Application of chitin- and chitosan-based materials for enzyme immobilizations: a review. Enzyme Microb Technol. 35:126–139.

Laurent S, Forge D, Port M, Roch A, Robic C, Vander Elst L, Muller RN. 2008. Magnetic iron oxide nanoparticles: synthesis, stabilization, vectorization, physicochemical characterizations, and biological applications. Chem Rev. 108:2064–2110.

Li D, Luo L, Pang Z, Ding L, Wang Q, Ke H, Huang F, Wei Q. 2014. Novel phenolic biosensor based on a magnetic polydopamine-laccase-nickel nanoparticle loaded carbon nanofiber composite. ACS Appl Mater Interfaces. 6:5144–5151.

Li Y, Qin C, Chen C, Fu Y, Ma M, Xie Q. 2012. Highly sensitive phenolic biosensor based on magnetic polydopamine-laccase-Fe_3O_4 bionanocomposite. Sens Actuat B Chem. 168:46–53.

Li Y, Zhang L, Li M, Pan Z, Li D. 2012. A disposable biosensor based on immobilization of laccase with silica spheres on the MWCNTs-doped screen-printed electrode. Chem Cent J. 6:103.

Liu Y, Qu X, Guo H, Chen H, Liu B, Dong S. 2006. Facile preparation of amperometric laccase biosensor with multifunction based on the matrix of carbon nanotubes-chitosan composite. Biosens Bioelectron. 21:2195–2201.

Mazur M, Krywko-Cendrowska A, Krysinski P, Rogalski J. 2009. Encapsulation of laccase in a conducting polymer matrix: a simple route towards polypyrrolemicrocontainers. Synth Met. 159:1731–1738.

Osaka T, Matsunaga T, Nakanishi T, Arakaki A, Niwa D, Iida H. 2006. Synthesis of magnetic nanoparticles and their application to bioassays. Anal Bioanal Chem. 384:593–600.

Piontek K, Antorini M, Choinowski T. 2002. Crystal structure of a laccase from the fungus Trametes versicolor at 1.90-A resolution containing a full complement of coppers. J Biol Chem. 277:37663–37669.

Podzus PE, Daraio ME, Jacobo SE. 2009. Chitosan magnetic microspheres for technological applications: preparation and characterization. Phys B. 404:2710–2712.

Sanchez-Avila J, Fernandez-Sanjuan M, Vincente J, Lacorte S. 2011. Development of a multi-residue method for the determination of organic micropollutants in water, sediment and mussels using gas chromatography-tandem mass spectrometry. J Chromatogr A. 1218:6799–6811.

Sarika C, Rekha K, Narasimha Murthy B. 2015a. Studies on enhancing operational stabilityof a reusable laccase-based biosensor probefor detection of ortho-substituted phenolicderivatives. 3 Biotech. 5:1–14.

Sarika C, Rekha K, Narasimha Murthy B. 2015b. Immobilized laccase-based biosensor for the detection of disubstituted methyl and methoxy phenols – application of Box–Behnken design with response surface methodology for modeling and optimization of performance parameters. Artif Cells Nanomed Biotechnol. [Epub ahead of print]. doi:10.3109/21691401.2015.1096793.

Schweigert N, Zehnder AJ, Eggen R. 2001. Chemical properties of catechols and their molecular modes of toxic action in cells, from microorganisms to mammals. Environ Microbiol. 3:81–91.

Sharma H, Mutharasan R. 2013. Review of biosensors for foodborne pathogens and toxins. Sens Actuat B Chem. 183:535–549.

Silverstein RM, Webster FX, Kiemle DJ. 2005. Spectrometric Identification of Organic Compounds. 7th ed. New York: John Wiley & Sons.

Downloaded by [Orta Dogu Teknik Universitesi] at 17:21 12 April 2016

Sołoducho J, Cabaj J. 2013. Phenolic compound hybrid detectors. J Biomater Nanobiotechnol. 4:17–27.

Song MJ, Kim JH, Lee SK, Lee JH, Lim DS, Hwang SW, Whang D. 2010. Pt-polyaniline nanocomposite on boron-doped diamond electrode for amperometic biosensor with low detection limit. Microchim Acta. 171:249–255.

Umar A, Ahmad R, Hwang SW, Kim SH, Al-Hajry A, Hahn YB. 2014. Development of highly sensitive and selective cholesterol biosensor based on cholesterol oxidase co-immobilized with α-Fe_2O_3 micro-pine shaped hierarchical structures. Electrochim Acta. 135:396–403.

Valentini F, Palleschi G. 2008. Nanomaterials and analytical chemistry. Anal Lett. 41:479–520.

Xu J, Yang H, Fu W, Du K, Sui Y, Chen J, et al. 2007. Preparation and magnetic properties of magnetite nanoparticles by sol-gel method. J Magn Magn Mater. 309:307–311.

Xu X, Lu P, Zhou Y, Zhao Z, Guo M. 2009. Laccase immobilized on methylene blue modified mesoporous silica MCM-41/PVA. Mater Sci Eng C. 29:2160–2164.

Xuan S, Wang YXJ, Yu JC, Leung KCF. 2009. Tuning the grain size and particle size of superparamagnetic Fe_3O_4 microparticles. Chem Mater. 21:5079–5087.

Yao Y, Shiu KK. 2007. Electron-transfer properties of different carbon nanotube materials and their use in glucose biosensors. Anal Bioanal Chem. 387:303–309.

Zboril R, Mashlan M, Petridis D. 2002. Iron (III) oxides from thermal processes-synthesis, structural and magnetic properties, Mossbauer spectroscopy characterization, and applications. Chem Mater. 14:969–982.

Zhang Y, Gui Y, Wu X, Feng H, Zhang A, Wang L, Xia T. 2009. Preparation of nanostructures NiO and their electrochemical capacitive behaviors. Int J Hydrogen Energy. 34:2467–2470.

Zhao Z, Lei W, Zhang X, Wang B, Jiang H. 2010. ZnO-based amperometric enzyme. Sensors. 10:1216–1231.

Zhou XH, Liu LH, Bai X, Shi HC. 2013. A reduced graphene oxide based biosensor for high-sensitive detection of phenols in water samples. Sens Actuat B Chem. 181:661–667.

Downloaded by [Orta Dogu Teknik Universitesi] at 17:21 12 April 2016